Inorganic Chemistry

ARTICLE

pubs.acs.org/IC

pH-Dependent Spectroscopic and Luminescent Properties, and Metal-Ion Recognition Studies of Re(I) Complexes Containing 2-(2′-Pyridyl)benzimidazole and 2-(2′-Pyridyl)benzimidazolate

Biing-Chiau Tzeng,*[,†] Bo-So Chen,[†] Chang-Kai Chen,[†] Yuan-Ping Chang,[†] Wen-Chian Tzeng,[†] Tsung-Yi Lin,[‡] Gene-Hsiang Lee,[‡] Pi-Tai Chou,*[,‡] Yu-Jie Fu,[§] and A. Hsiu-Hua Chang*[,§]

[†]Department of Chemistry and Biochemistry, National Chung Cheng University, 168 University Road, Min-Hsiung, Chiayi 62102, Taiwan

[‡]Department of Chemistry, National Taiwan University, 1, Sec. 4, Roosevelt Road, Taipei 10617, Taiwan

[§]Department of Chemistry, National Dong Hwa University, 1, Sec. 2, Da Hsueh Road., Shoufeng, Hualien 97401, Taiwan

Supporting Information

ABSTRACT: A series of Re(I) complexes, $[Re(CO)_3Cl(HPB)]$ (**1**), $[Re(CO)_3(PB)H_2O]$ (**2**), $[Re(CO)_3(NO_3)(PB\text{-}AuPPh_3)]$ (**3**), and $[Re(CO)_3(NO_3)(PB)Au(dppm\text{-}H)Au]_2$ (**4**) [HPB = 2-(2′-pyridyl)benzimidazole; dppm = 2,2′-bis(diphenylphosphinomethane)], have been synthesized and characterized by X-ray diffraction. Complex **1**, which exhibits interesting pH-dependent spectroscopic and luminescent properties, was prepared by reacting $Re(CO)_5Cl$ with an equimolar amount of 2-(2′-pyridyl)benzimidazole. The imidazole unit in complex **1** can be deprotonated to form the imidazolate unit to give complex **2**. Addition of 1 equiv of $AuPPh_3(NO_3)$ to complex **2** led to the formation of a heteronuclear complex **3**. Addition of a half an equivalent of $dppm(Au(NO_3))_2$ to complex **2** yielded **4**. In both **3** and **4**, the imidazolate unit acts as a multinuclear bridging ligand. Complex **4** is a rare and remarkable example of a Re_2Au_4 aggregate in combination with μ_3-bridging 2-(2′-pyridyl)benzimidazolate. Finally, complex **2** has been used to examine the Hg^{2+}-recognition event among group 12 metal ions. Its reversibility and selectivity toward Hg^{2+} are also examined.

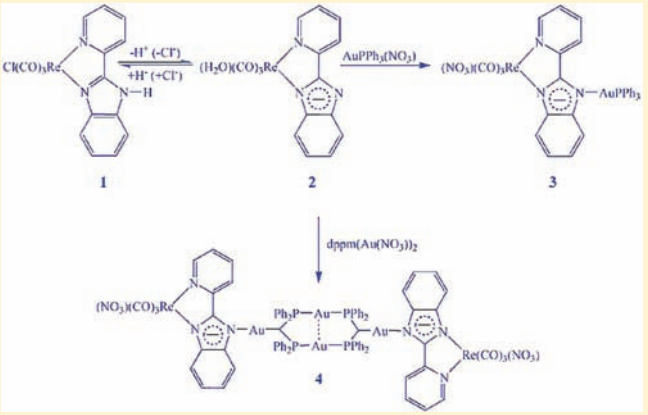

INTRODUCTION

Given characteristic metal-to-ligand charge-transfer (MLCT) excited states, rich luminescent Re(I)-bipyridine complexes have attracted considerable attention for their intriguing photophysical, photochemical, excited-state redox properties, and potential applications in light emitting devices.[1] Therefore, the widespread use of Re(I)-bipyridine complexes displaying the charge-transfer phosphorescence has resulted in the study of many diimine-type ligands. This is also because tuning the steric and electronic properties of "diimine analogues" is readily accessible by synthesis.[2] In this context, the 2-(2′-pyridyl)benzimidazole (HPB) ligand[3] and its derivatives[4] are not unusual in coordination compounds, but many of the reported complexes have been of interest because of the possibility of deprotonating the NH group of the imidazole unit, leading to the formation of an imidazolate unit (PB). Haga et al.[3a] first showed that the redox and spectroscopic properties of $[Ru(bpy)_2(HPB)]^{2+}$ were highly dependent on pH. Since the imidazole form is suggested to have a stronger π-donating ability than the imidazolate, they also demonstrated that $[Ru(bpy)_2(HPB)]^{2+}$ (bpy = 2,2′-bipyridine) shows ^{3}MLCT luminescence comparable to that of $[Ru(bpy)_3]^{2+}$ with a slight red-shift and a shorter lifetime,[3b] indicating that $[Ru(bpy)_2(HPB)]^{2+}$ also has rich luminescence. Indeed, the deprotonated form (PB) is able to act as a multinucleating bridging ligand with metal ions in assembled products. These complexes, composed of two or more redox- and photoactive components, display electronic communications between sites and can be anticipated to find useful applications in material science.

The selective recognition and sensing of biologically or environmentally important ions by artificial receptors has emerged as a key research topic in supramolecular chemistry. In this regard, the design and synthesis of receptors sensitive to ion−receptor interactions and capable of exhibiting either a chromogenic and/or a fluorogenic response are of current interest. Methodologies for the efficient detection and quantitative determination of ions are being developed, and a variety of

Received: September 17, 2010
Published: May 23, 2011

dx.doi.org/10.1021/ic1019058 | *Inorg. Chem.* 2011, 50, 5379–5388

molecular sensors for anions have been synthesized and designed in the past decade.[5] In this context, the Hg(II) ion is considered to be one of the most hazardous to environment and human health. Up to now, intensive efforts have been made to develop artificial receptors for the Hg(II) ion, and the fluorescence technique has been known to offer a promising approach for simple and rapid tracking of Hg(II) ions.[6] We report herein pH-dependent spectroscopic and luminescent properties of Re(I) complexes with HPB and PB ligands, and the evaluation of their sensing capabilities toward group 12 metal-ions.

EXPERIMENTAL SECTION

General Information. All reactions were performed under a nitrogen atmosphere. Solvents for syntheses (analytical grade) were purified by literature methods, and 2-(2′-pyridyl)benzimidazole (HPB), $Re(CO)_5Cl$, $M(ClO_4)_2$ ($M = Zn^{2+}$, Cd^{2+}, Hg^{2+}), and $Hg(NO_3)_2$ were obtained commercially and used without any further purification. NMR spectra were recorded on a Bruker DPX 400 MHz NMR spectrometer, and samples were prepared in deuterated solvents with the usual standards. Infrared (IR) spectra were recorded with samples in the form of KBr pellets on a Perkin-Elmer PC 16 FTIR spectrometer. UV/vis and steady-state emission spectra were recorded on Hitachi U-3010 and Hitachi F-7000 spectrophotometers, respectively. The powder X-ray diffraction (PXRD) data were recorded on a Shimadzu XRD-6000 diffractometer. Positive electrospray-ionization (ESI) mass spectra were obtained on a Q-Tof LC/MS/MS mass spectrometer. Elemental analysis (EA) of the complexes was performed on an Elementar vario EL III Heraeus CHNOS Rapid F002 elemental analyzer, and the solid samples were pretreated by subjecting them to a vacuum overnight. To determine the photoluminescence quantum yield in solution, the samples were degassed by three freeze−pump−thaw cycles. 4-(Dicyanomethylene)-2-methyl-6-(paradimethylaminostyryl)-4H-pyran (DCM, λ_{max} = 615 nm, Exciton) in methanol, with a quantum yield of ∼0.4, served as the standard for measuring the quantum yield. Solid-state quantum yields were determined with a calibrated integrating sphere system. The uncertainty of the quantum yield measurement was in the range of <2% (an average of three replica). Lifetime studies were performed with an Edinburgh FL 900 photon-counting system, using a hydrogen-filled lamp as the excitation source. The emission decays were fitted by the sum of exponential functions with a temporal resolution of ∼300 ps by the deconvolution of instrument response function.

Synthesis. *$[Re(CO)_3Cl(HPB)]$ (**1**).* A 36.1 mg portion (0.1 mmol) of $Re(CO)_5Cl$ and 19.5 mg (0.1 mmol) of HPB in 10 mL of toluene were heated with stirring at 60 °C for 24 h, whereupon a pale yellow solid was formed. After cooling, the solid was collected on a glass frit, washed with hexanes, dried under a vacuum, and weighed (ca. 80% yield). Yellow single crystals were obtained by crystallization from CH_2Cl_2/diethyl ether. ^1H NMR (400 MHz, $CDCl_3$): δ 7.27 [m, 2H, Ph/Py], 7.34 [m, 2H, Ph/Py], 7.79 [d, J = 7.6 Hz, 1H, Ph/Py], 7.86 [m, 1H, Ph/Py], 8.20 [d, J = 8.0 Hz, 1H, Ph/Py], 8.87 [d, J = 5.2 Hz, 1H, Ph/Py], 13.72 [s, 1H, N*H*]. FT-IR: ν_{NH} = 3039 cm^{-1}, $\nu_{C\equiv O}$ = 2,024 and 1898 cm^{-1}, $\nu_{C=N/C=O}$ = 1608 and 1483 cm^{-1}. ESI-MS: $[M - Cl]^+$, m/e = 501.0, 10%. Anal. Calcd (%) for $C_{15}H_9ClN_3O_3Re$: C, 35.97; H, 1.81; N, 8.39. Found (%): C, 36.29; H, 1.80; N, 8.43.

*$[Re(CO)_3(PB)H_2O]$ (**2**).* A methanolic solution of $[Re(CO)_3Cl(HPB)]$ (50.3 mg, 0.1 mmol) was stirred for 20 min in the presence of NaOH (4.8 mg, 0.1 mmol). MeOH was then removed on a rotary evaporator. Deionized water (20 mL) was added to the solid, and the pale yellow solid was collected on a glass frit, washed with hexanes, dried under a vacuum, and weighed (ca. 75% yield). Yellow single crystals were obtained by crystallization from tetrahydrofuran (THF)/dimethylsulfoxide (DMSO)/diethyl ether. ^1H NMR (400 MHz, DMSO-d_6): δ 7.14 [m, 1H, Ph/Py], 7.21 [m, 1H, Ph/Py], 7.61 [m, 1H, Ph/Py], 7.65 [d, J = 8.28 Hz, 1H, Ph/Py], 8.24 [m, 2H, Ph/Py], 8.35 [d, J = 7.96 Hz, 1H, Ph/Py], 8.90 [d, J = 5.4 Hz, 1H, Ph/Py]. FT-IR: $\nu_{C\equiv O}$ = 2,019 and 1888 cm^{-1}, $\nu_{C=N/C=O}$ = 1611 and 1461 cm^{-1}. ESI-MS: $[M + H^+ - H_2O]^+$, m/e = 465.9, 100%. Anal. Calcd (%) for $C_{15}H_{10}N_3O_4Re$: C, 37.34; H, 2.09; N, 8.71. Found (%): C, 37.21; H, 2.18; N, 8.58.

*$[Re(CO)_3(NO_3)(PB\text{-}AuPPh_3)]$ (**3**).* To a solution of $Au(PPh_3)NO_3$ {obtained by treating $Au(PPh_3)Cl$ (52 mg, 0.1 mmol) with $AgNO_3$ (20.4 mg, 0.12 mmol)} in CH_2Cl_2/MeOH (1:1, 30 mL) was added **2** (48.3 mg, 0.1 mmol). After stirring for 1 h, the solution became pale yellow. The solution was then reduced to 5 mL volume on a rotary evaporator, and the yellow solid was obtained upon addition of diethyl ether with about 72% yield. Yellow single crystals were obtained by crystallization from CH_2Cl_2/diethyl ether. ^1H NMR (400 MHz, DMSO-d_6): δ 7.31 [m, 1H, Ph/Py], 7.46 [m, 2H, Ph/Py], 7.71 [m, 15H, PPh_3], 7.82 [m, 1H, Ph/Py], 8.12 [m, 2H, Ph/Py], 9.10 [m, 1H, Ph/Py], 9.27 [d, 1H, Ph/Py]. FT-IR: $\nu_{C\equiv O}$ = 2018 and 1892 cm^{-1}, $\nu_{C=N/C=O}$ = 1608 and 1473 cm^{-1}, and ν_{N-O} = 1279 cm^{-1}. ESI-MS: $[M - NO_3]^+$, m/e = 924.1, 20%. Anal. Calcd (%) for $C_{33}H_{23}AuN_4O_6PRe$: C, 40.21; H, 2.35; N, 5.68. Found (%): C, 40.38; H, 2.18; N, 5.58.

*$[Re(CO)_3(NO_3)(PB)Au(dppm\text{-}H)Au]_2$ (**4**).* To a solution of $dppm(AuNO_3)_2$ {obtained by treating $dppm(AuCl)_2$ (42.4 mg, 0.05 mmol) with $AgNO_3$ (20.4 mg, 0.12 mmol)} in CH_2Cl_2/MeOH (1:1, 40 mL) was added **2** (48.3 mg, 0.1 mmol). After stirring for 24 h the solution became pale yellow-green. The solution was then reduced to 5 mL volume on a rotary evaporator, and the yellow-green solid was obtained upon addition of diethyl ether with about 54% yield. Yellow-green single crystals were obtained by crystallization from THF/DMSO/DMF/diethyl ether. FT-IR: $\nu_{C\equiv O}$ = 2021 and 1892 cm^{-1}, $\nu_{C=N/C=O}$ = 1610 and 1466 cm^{-1}, and ν_{N-O} = 1279 cm^{-1}. ESI-MS: $[M - 2NO_3]^{2+}$, m/e = 1241.98, 7.5%; $[M - 2NO_3]\cdot 2CH_3CN\}^{2+}$, m/e = 1282.99, 47.0%. Anal. Calcd (%) for $C_{80}H_{58}Au_4N_8O_{12}P_4Re_2$: C, 36.85; H, 2.24; N, 4.30. Found (%): C, 36.59; H, 2.36; N, 4.45.

X-ray Crystallography. Suitable crystals were mounted on glass capillaries. Data collection was carried out on a Bruker SMART CCD diffractometer with Mo radiation (0.71073 Å) at 150 and 100 K for complexes **1**−**3** and **4**, respectively. A preliminary orientation matrix and unit cell parameters were determined from 3 runs of 15 frames each, each frame corresponding to 0.3° scan in 20 s, followed by spot integration and least-squares refinement. Data were measured using an ω scan of 0.3° per frame for 20 s until a complete hemisphere had been collected. Cell parameters were retrieved using SMART[7a] software and refined with SAINT[7b] on all observed reflections. Data reduction was performed with the SAINT software and corrected for Lorentz and Polarization effects. Absorption corrections were applied with the program SADABS.[7c] The structure was solved by direct methods with the SHELXS-97[7d] program and refined by full-matrix least-squares methods on F^2 with SHELXL-97.[7e] All non-hydrogen atomic positions were located in difference Fourier maps and refined anisotropically. Hydrogen atoms were constrained to the ideal geometry using an appropriate riding model. Detailed data collection and refinement of complexes **1**−**4** is summarized in Table 1.

Theoretical Method. The density functional B3LYP[8a,b]/LanL2DZ[8c] calculations were performed for monomers of the Re(I) complexes **1**−**4** in the corresponding crystal geometries. The Gaussian 03 program.[9] was utilized in the electronic structure calculations.

RESULTS AND DISCUSSION

The Re(I) 2-(2′-pyridyl)benzimidazole complex (**1**) has been synthesized by reacting $Re(CO)_5Cl$ with an equimolar amount of 2-(2′-pyridyl)benzimidazole in toluene at 60 °C for 24 h with a yield of about 80%. Complex **1** was characterized by the X-ray diffraction, and was found to have the imidazole unit acting as a

Table 1. Crystallographic data of 1, 2·THF, 3·CH_2Cl_2, and 4

	1	2·THF	3·CH_2Cl_2	4
empirical formula	$C_{15}H_9ClN_3O_3Re$	$C_{19}H_{18}N_3O_5Re$	$C_{34}H_{25}AuCl_2N_4O_6PRe$	$C_{80}H_{56}Au_4N_8O_{12}P_4Re_2$
formula weight	500.9	554.56	1070.62	2605.47
crystal system	triclinic	monoclinic	triclinic	triclinic
space group (No.)	$P\bar{1}$	$P2_1/c$	$P\bar{1}$	$P\bar{1}$
a (Å)	7.6232(2)	6.9427(1)	10.7751(2)	12.950(2)
b (Å)	8.4654(2)	14.2672(2)	11.4767(2)	13.243(2)
c (Å)	11.8430(3)	19.3829(3)	14.8100(3)	14.050(3)
α (deg)	90.7883(13)	90	79.0817(12)	61.944(2)
β (deg)	95.1188(15)	99.8492(7)	75.7238(10)	89.385(4)
γ (deg)	92.0589(16)	90	82.9814(12)	84.796(3)
V (Å^3)	760.62(3)	1891.63(5)	1737.27(6)	2116.2(6)
Z	2	4	2	2
F(000) (e)	472	1072	1016	1214
μ (Mo−Kα) (mm^{-1})	8.181	6.460	7.949	9.892
reflections collected	11153	10751	25421	20272
independent reflections	3456 (R_{int} = 0.070)	4300 (R_{int} = 0.041)	7950 (R_{int} = 0.068)	7550 (R_{int} = 0.026)
observed reflections ($F_o \geq 2\sigma(F_o)$)	3456	4300	7950	7550
refined parameters	208	253	443	662
goodness-of-fit on F^2	1.002	1.005	1.071	1.117
R^a, R$_w$^{b} ($I \geq 2\sigma(I)$)	0.038, 0.075	0.029, 0.057	0.039, 0.091	0.043, 0.103
R^a, R$_w$^{b} (all data)	0.054, 0.081	0.045, 0.062	0.060, 0.103	0.050, 0.105

^{a} $R = \Sigma||F_o| - |F_c||/\Sigma|F_o|$. ^{b} $wR_2 = \{\Sigma w(F_o^2 - F_c^2)^2/\Sigma w(F_o^2)^2\}^{1/2}$.

Scheme 1

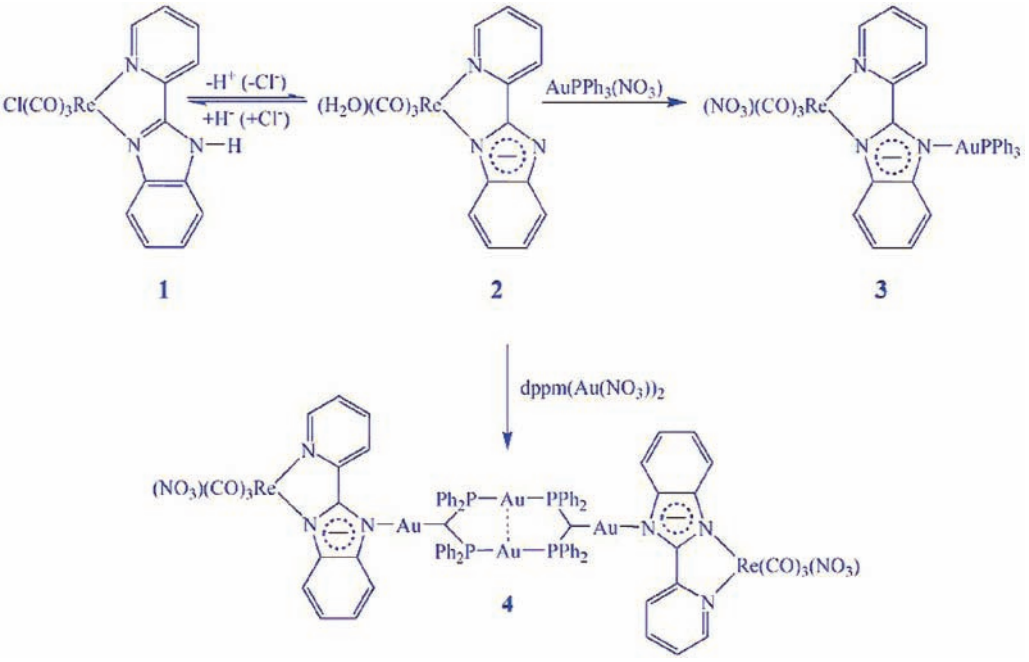

chelate. The imidazole ligand in complex **1** can be deprotonated to form the imidazolate unit to give complex **2**. The addition of 1 equiv of $AuPPh_3(NO_3)$ to complex **2** led to the formation of a heteronuclear complex **3**. On the other hand, the addition of a half equivalent of $dppm(Au(NO_3))_2$ to complex **2** generated **4**. Scheme 1 shows the synthesis of complexes **2**−**4** from complex **1**. Indeed, complex **1** has been shown to have pH-dependent spectroscopic and luminescent properties, and its deprotonated form (**2**) with the imidazolate unit is expected to act as a multinuclear bridging ligand in the assembly process. In addition, complex **2** is also evaluated for group 12 metal-ion sensing events.

dx.doi.org/10.1021/ic1019058 |*Inorg. Chem.* 2011, 50, 5379–5388

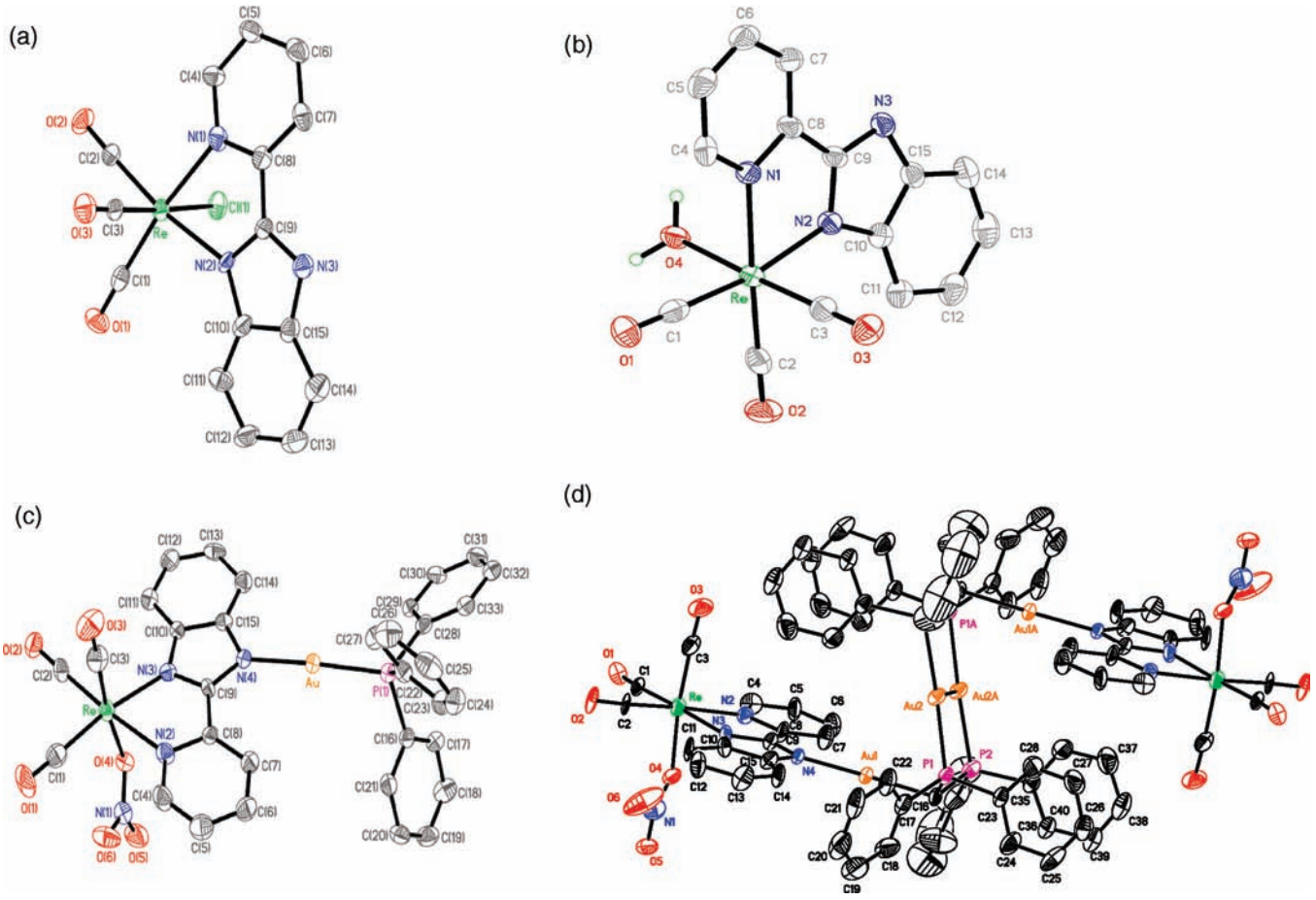

Figure 1. Molecular structure of **1** (a), **2** (b), **3** (c), and **4** (d). ORTEP diagram shows 50 and 30 % probability ellipsoids for **1**−**3** and **4**, respectively.

Description of Crystal Structure of Complexes 1−4. Perspective views of complexes **1**−**4** are shown in Figure 1a−d, respectively. Each complex has a very similar coordination geometry about the Re(I) ion, with a *fac*-tricarbonyl arrangement and a pseudo-octahedral geometry. Among complexes **1**−**4**, the values of Re−$N_{pyridyl}$ (2.193(5)−2.226(9) Å) are in general slightly longer than those of Re−$N_{imidazole/imidazolate}$ (2.142(3)−2.153(11) Å) and the bite angles of the chelating imidazole/imidazolate ligands are within 74−75°, which are all in agreement with the trend reported in refs 3c,4. Since the N(2)−C(9)/N(3)−C(9) distances in the imidazole units are 1.334(7)/1.344(7) Å and 1.350(5)/1.332(5) Å for complexes **1** and **2**, respectively, the partial delocalization between single and double bonds can be observed, which are different from those of localized forms found in Re(I) alkyl-imidazole complexes. However, the N(3)−C(9) and N(4)−C(9) distances are 1.316(7) and 1.353(7) Å, respectively, in complex **3**, indicative of less delocalization in the imidazolate unit. The imidazolate unit acts as a μ_3-bridging form, and chelates not only to a Re(I) ion, but also bridges to a $AuPPh_3^+$ unit in complex **3**. Therefore, the conclusion is that the imidazole and imidazolate units in complexes **1** and **2** are delocalized, whereas the alkyl-imidazole and $AuPPh_3$-imidazolate in complex **3** are more localized.[4a] This finding may be ascribed to the similar electronic effect of the alkyl and $AuPPh_3^+$ units, which are not the same as the H^+ unit. In addition, $\pi\cdots\pi$ interactions are also found in the crystal lattices of complexes **1** and **2**, and such interactions did increase the structural dimensions of the 2-D (the $\pi\cdots\pi_{centroid}$ distance of 3.655 Å between two parallel phenyl rings)[10] and 1-D (the $\pi\cdots\pi_{centroid}$ distance of 3.736 Å between two phenyl rings with a dihedral angle of 5.8°)[10] frameworks for complexes **1** and **2**, respectively. Since a flipping disorder occurs in the imidazolate unit in complex **4**, discussions regarding bond parameters of the imidazolate unit are not possible.

Except for the imidazole and imidazolate units, the other bond parameters about the Re(I) ions of complexes **1**−**4** are not uncommon, with respect to the reported Re(I) alkyl-imidazole complexes.[4] However, heteronuclear complexes **3** and **4** have the imidazolate unit acting as a μ_3-bridging form, which is a rare phenomenon in the literature. In complex **3**, the imidazolate unit chelates to the Re(I) ion and also bridges to the $AuPPh_3^+$ group with a Au−$N_{imidazolate}$ distance of 2.051(5) Å and a P−Au−N angle of 176.39(15)°, which are comparable to the related values of 2.075(4) Å and 176.39(15)° in $[HPB(AuPPh_3)]ClO_4$,[3c] respectively. Surprisingly, a novel heteronuclear aggregate, namely, complex **4**, has been serendipitously isolated and characterized by X-ray diffraction. It has a $dppm_2Au_2$ unit as a core structure with an intramolecular Au(I)···Au(I) distance of 2.9814(7) Å, where each methylene group in dppm is singly deprotonated to coordinate to the Au(I)-imidazolate-Re(I) group. Although the deprotonated methylene group coordinating to the metal ion is not unusual,[11] the Re_2Au_4 aggregate is a remarkable example in the literature. Although the mechanism is so far unclear, the infrared spectral data show that the complexes

dx.doi.org/10.1021/ic1019058 |*Inorg. Chem.* 2011, 50, 5379–5388

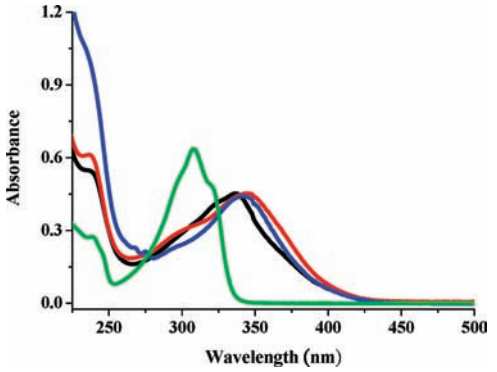

Figure 2. Absorption spectra of **1** (black line), **2** (red line), **3** (blue line), and HPB (green line) are measured in CH_3OH at a concentration of 2.5×10^{-5} M, respectively.

isolated after 1 h and 24 h of reaction, and single crystals are all highly similar (see Supporting Information, Figure S1). This indicates that complex **4** is not formed in the crystal-growth process, but most likely formed directly from the reaction. A $\pi\cdots\pi$ interaction is also found in complex **4** between two phenyl rings in dppm (the $\pi\cdots\pi_{centroid}$ distance of 3.618 Å and a dihedral angle of 9.8°).[10] Additionally, the Cl^- anions on Re(I) ions in complexes **3** and **4** have both been displaced by the NO_3^- anions in the reaction process.

Photophysical Properties. In general, all complexes **1**−**3** measured in CH_3OH show an absorption band at about 237 nm, a shoulder at about 300 nm, and also broad bands at about 336, 342, and 345 nm, respectively (Figure 2). On the basis of the similarity to the absorptions at about 239 and 308 nm with two shoulders at 300 and 321 nm of HPB, these absorptions are most likely ascribed to intraligand (IL) transitions. However, the absorption bands at 336−345 nm have low-energy absorptions tailing to about 450 nm, where a characteristic MLCT transition at about 380 nm possibly sits under this region. For reference, the absorption spectrum of the Re(I) ethyl-imidazole complex[4a] shows an absorption maximum at about 400 nm assigned to a characteristic MLCT transition, which is expected to be solvent-dependent. Therefore, a series of solvent-dependent absorption spectra of **1** have been also measured in CH_2Cl_2, $CHCl_3$, THF, CH_3OH, CH_3CN, and DMSO (see Supporting Information, Figure S2). Despite similar absorption features for low-energy absorptions at about 380 nm tailing to 450 nm, a distinctly different spectral feature can be observed at about 285−350 nm. It seems like that MLCT absorption is red-shifted in the non-hydrogen bonding solvents such as in CH_2Cl_2, $CHCl_3$, and CH_3CN relative to those of hydrogen-bonding solvent like DMSO and MeOH. A similar phenomenon is observed in the emission spectra and will be discussed later. Note that in Figure 2, the slight red shifts in the absorption energies from **1** to **3**, or to **2** in CH_3OH may be due to increased conjugation in the imidazolate unit compared with the imidazole. Because of the poor solubility of crystalline samples of complex **4**, its absorption and luminescence measurements in solution were not possible.

All emission spectra of complexes **1**−**4** in the solid state and complexes **1**−**3** in CH_3OH have been measured; their spectra are shown in Figures 3a−c. Upon photoexcitation at 380 nm at room temperature, solid samples of complexes **1**, **2**, and **3** show low-energy emission bands at about 560, 532, and 556 nm, respectively, as shown in Figure 3a. Their respective excitation

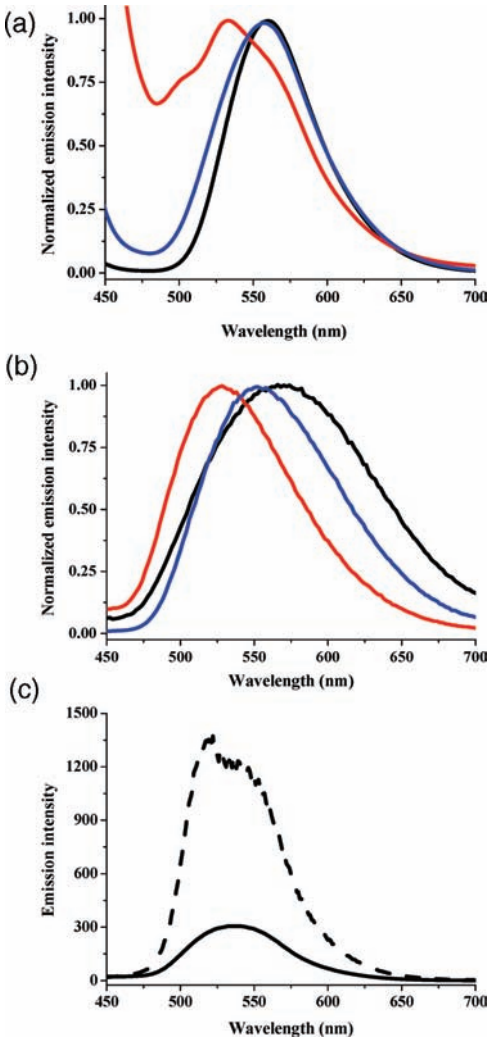

Figure 3. Emission spectra of **1** (black line), **2** (red line), and **3** (blue line) measured (a) in the solid state and (b) in CH_3OH at a concentration of 2.5×10^{-5} M, respectively. (c) The emission spectra of **4** measured in the solid state at room temperature (solid line) and at 77 K (dash line). Excitation wavelength was used at 380 nm.

spectra are shown in Supporting Information, Figure S3. In solution such as CH_3OH, the emission spectra for complexes **1**−**3** show emission bands at about 576, 528, and 553 nm, respectively (Figure 3b). Similar to the absorption spectra, complex **1** shows solvent-dependent emission, with peak wavelength varied in a variety of solvents such as CH_2Cl_2, $CHCl_3$, THF, CH_3OH, CH_3CN, and DMSO, being at 590, 590, 610, 576, 606, and 578 nm, respectively (see Supporting Information, Figure S4, vide infra).

Emission lifetime and quantum yield measurements are also performed and pertinent data are listed in Table 2. According to Table 2, the radiative decay rate constant, k_r, can be derived by the equation $k_r = k_{obs} \times \Phi = 1/\tau \times \Phi$. As a result, the k_r value is deduced to be in the range of 10^4−10^5 s^{-1} for the titled compounds, clearly indicating that the emission originates from a triplet manifold, that is, the phosphorescence. As for the control experiment, the free ligand HPB in CH_3OH exhibits dual emission maxima at 422 and 538 nm (see Supporting Information, Figure S5). While the 422 nm emission, which is a mirror

dx.doi.org/10.1021/ic1019058 |*Inorg. Chem.* 2011, 50, 5379–5388

Table 2. Emission Lifetime and Quantum Yield Data of Complexes 1−3, where Φ, τ, k_r, and k_{nr} stand for Quantum Yield, Lifetime, Radiative and Nonradiative Decay Rate Constants, Respectively

	emission/nm	Φ	τ (μs)	k_r	k_{nr}
			CH_2Cl_2		
1	590	0.031	0.075	4.1×10^5	1.3×10^7
2	542	0.004	0.042	9.5×10^4	2.4×10^7
3	568	0.009	0.176	5.1×10^4	5.6×10^6
			MeOH		
1	576	0.046	0.087	5.3×10^5	1.1×10^7
2	528	0.006	0.085	7.0×10^4	1.2×10^7
3	553	0.016	0.222	7.2×10^4	4.4×10^6

image with respect to the absorption spectrum, is ascribed to the normal Stokes shifted emission of HPB, the large Stokes shifted emission (with respect to the absorption peak) originates from the excited state proton transfer reaction assisted by the methanol molecule. It has been reported that in methanol HPB exists predominantly as a polysolvated form (by methanol molecules).[12,13] Upon electronic excitation, the solvent reorganization takes place within the lifespan of the excited state (S_1). Once it forms a CH_3OH/HPB cyclic hydrogen bonded complex fast proton transfer takes place through a proton relay assisted by CH_3OH, resulting in the proton-transfer tautomer (see Scheme S1 in Supporting Information for detailed mechanism). The solvent reorganization to the monocyclic solvated form is an endergonic process. Therefore, the rate of $S_1 \rightarrow S_0$ normal emission competes with the rate of thermally activated proton transfer, giving rise to both normal and proton-transfer tautomer emission for HPB in CH_3OH. Because of the lack of proton donating property, excited-state proton transfer was not observed for HPB in aprotic solvents. Thus, only normal emission can be resolved in, for example, CH_2Cl_2 or CH_3CN. More importantly, it should be noted that once both diimine sites have been involved in coordination with Re(I) such as complexes **1**−**4**, proton transfer is prohibited because of the lack of a proton accepting site. Therefore, there should be no proton transfer emission for complexes **1**−**4** in any solvents and solid state.

Along the above line, the emission of **1**−**4** with peak wavelength >500 nm cannot be assigned to the ligand (HPB) emission solely; otherwise it would be in the range of 400−450 nm. More plausibly, for complexes **1**−**3** the phosphorescence is ascribed to the MLCT origin mixed, to a certain extent, with the IL character in the triplet manifold. Supplementary support of this viewpoint is given by the computational approach. Figure 4 shows the HOMO and LUMO frontier orbitals for complexes **1**−**4** involved in the lowest lying transition in both singlet and triplet manifolds. Clearly, the HOMO of **1**−**3** is mainly located at both d_π of Re(I) and π orbitals of imidazolate, with a larger proportion for the latter, while the LUMO of complexes (**1**), (**2**), and (**3**) are rather similar and all stem predominately from the ligands. Accordingly, the assignment of the phosphorescence to MLCT and IL transitions is unambiguous. As for complex **4**, the calculation shows that HOMO and LUMO belong to the Re(I) d_π and two interacting Au(I) metal (plus few in phosphorus atom), respectively. In other words, if the calculation is trustable, the lowest lying transition of complex

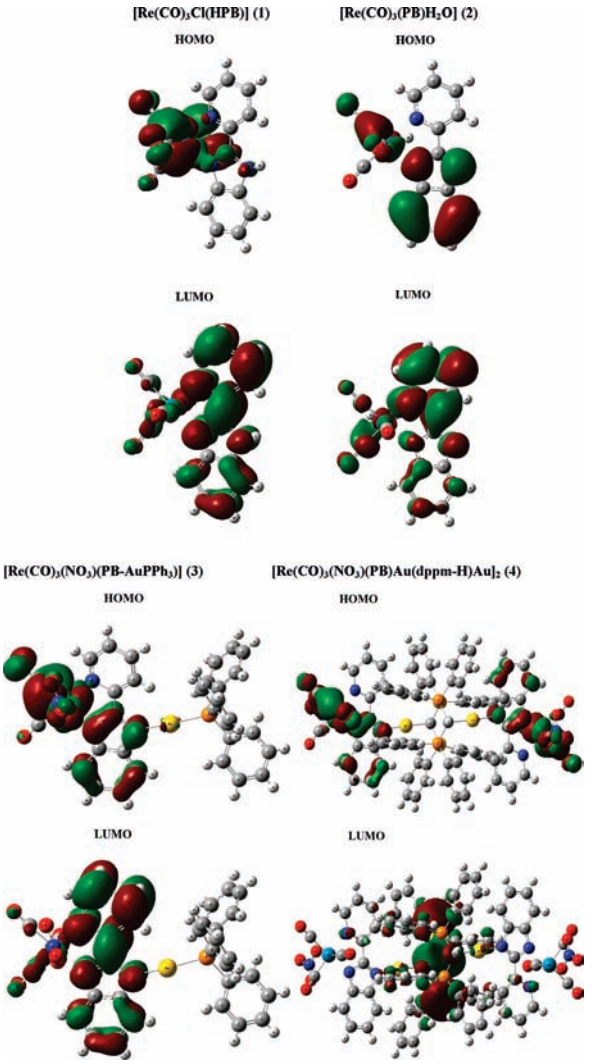

Figure 4. Calculated frontier orbitals of HOMO and LUMO for complexes **1**−**4**.

4 mainly involves metal Re(I) → Au(I) transition. Accordingly, the emission property of complex **4** seems to be different from that of complexes **1**−**3**. Nevertheless, because of the system complexity like **4**, large uncertainty may be raised in the calculation, so that one should not take the result into serious account. A more advanced calculation should be performed to resolve this issue. Interestingly, in solid, complex **4** emits at about 536 nm at room temperature and at 77 K as shown in Figure 3c. We are a little bit surprised that the low-energy MLCT (a Re-diimine chromophore)[3,4] and/or MC (a short Au(I)···Au(I) contact),[14,15] which are most likely present in solution and often are dominant emissions in the literature, are not found for complex **4**.

With ample information provided above, the solvent dependent emission spectra for complex **1** can thus be discussed. According to the frontier orbital analysis (Figure 4), evidently, the major electron distribution for the lowest lying transition involves metal (d_π) (HOMO)→ to π^* (LUMO, delocalized in the entire 2-(2′-pyridyl)benzimidazole moiety) transition, namely, a type of MLCT. Thus, the change of dipole moment between ground and excited states (T_1 state for the emission) is

dx.doi.org/10.1021/ic1019058 |Inorg. Chem. 2011, 50, 5379–5388

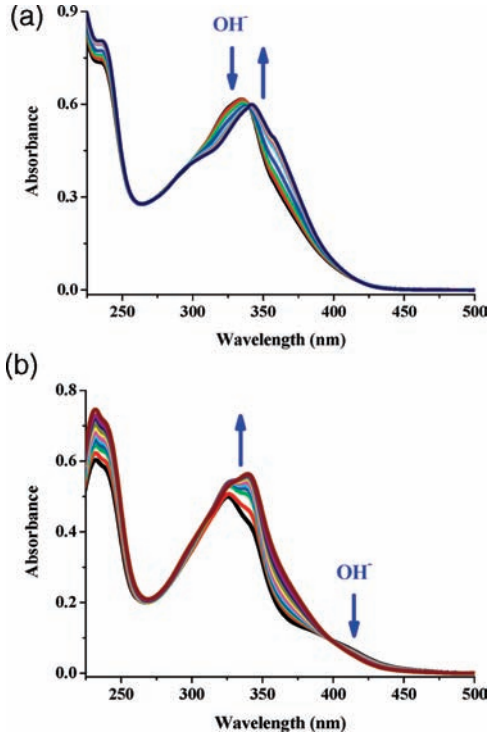

Figure 5. Absorption spectra of complex **1** at a concentration of 3.5×10^{-5} M upon stepwise addition of NaOH in (a) CH_3OH with 0 (pH = 6.13), 0.25 (6.60), 0.5 (6.95), 0.75 (7.29), 1 (7.53), 2 (8.11), 3 (8.48), 4 (8.70), and 5 (8.85) equiv of NaOH added and (b) CH_2Cl_2 (with 5% CH_3OH) with 0, 0.25, 0.5, 0.75, 1, 2, 3, 4, 5, 6, and 7 equiv of NaOH added.

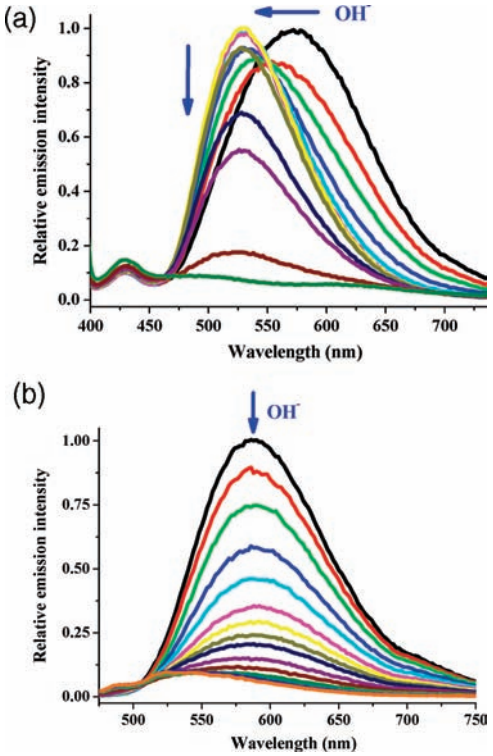

Figure 6. Emission spectra of complex **1** at a concentration of 3.5×10^{-5} M upon stepwise addition of NaOH in (a) CH_3OH with 0 (pH = 6.13), 0.2 (6.47), 0.4 (6.81), 0.6 (7.10), 0.8 (7.37), 1 (7.53), 2 (8.11), 3 (8.48), 4 (8.70), 5 (8.85), 10 (9.83), and 20 (10.85) equiv of NaOH added and (b) CH_2Cl_2 (with 5% CH_3OH) with 0, 0.2, 0.4, 0.6, 0.8, 1, 2, 3, 4, 5, 6, 7, 8, 9, and 10 equiv of NaOH added. Excitation wavelength was used at 380 nm.

expected. Because of the MLCT character, the dipole moment seems to be increased, which is subject to more solvent stabilization in the excited state, resulting in the red shift of the emission upon increasing solvent polarity. Such a red-shifted emission can be seen by the increase of emission peak wavelength from CH_2Cl_2 to CH_3CN. However, an opposite effect was also observed for the solvents that can provide proton accepting sites, such as THF, DMSO, and CH_3OH, which are believed to form hydrogen bond with imidazole N−H proton, giving the spectral blue shift. The combination of polarity and hydrogen-bonding effects is complicated, which is counterbalanced to give the anomalous solvent dependent emission spectra shown in Supporting Information, Figure S4.

Before wrapping up this section of fundamental of photophysics, we like to point out that for all complexes **1**−**3**, the phosphorescence quantum yield is low, as also supported by the large radiationless decay rate constant k_{nr} shown above. The fast nonradiative decay pathway seems independent of the ancillary ligand such as -Cl, -H_2O, or -NO_3. Alternatively, the five membered-ring coordination together with two dative bonds (cf. the ionic coordination) of the 2-(2′-pyridyl)benzimidazole moiety may cause the weakness of the metal−ligand bond, which gives a shallow potential energy surface (PES) that intersects with the ground state PES, resulting in dominant nonradiative deactivation.[16]

pH-Dependent Absorption and Luminescence. Since the imidazole and imidazolate units can be interconverted depending on the pH value of the solution, the spectroscopic and luminescent properties are therefore dependent on the ligand form adopted in Re(I) complexes. Thus, we set out to investigate this pH-dependent behavior. The pH-dependent absorption spectra of complex **1** upon stepwise addition of NaOH in CH_3OH and CH_2Cl_2 (with 5% CH_3OH) are shown in Figures 5a−b as representative examples, respectively. Addition of NaOH to a methanolic solution of complex **1** caused the original absorption maximum at 336 nm to be red-shifted and finally stabilized at 342 nm, with an isosbestic point at 340 nm, which is exactly the same as that of complex **2**. As mentioned in the last section the above red-shift in the absorption energy is ascribed to the increased conjugation in the imidazolate unit compared with the imidazole. Upon addition of HCl to a methanolic solution of complex **2**, the absorption maximum was blue-shifted to the original position at 336 nm (see Supporting Information, Figure S6) indicating that this pH-dependent behavior is reversible. The absorption titration carried out in CH_2Cl_2 (with 5% CH_3OH) was slightly different from that in CH_3OH. Upon addition of NaOH, the absorptions at 326−400 nm increase concomitantly with a slight decrease at 400−500 nm, with an isosbestic point at 400 nm. Addition of HCl to a solution of complex **2** caused the absorptions at 326−400 nm to decrease and the absorptions at 400−500 nm slightly to increase, and finally back to the original position (see Supporting Information, Figure S7). The above results indicate that the pH-dependent behavior in either solvent is reversible.

For the luminescence titration, stepwise addition of NaOH to a methanolic solution of complex **1** causes the original emission

dx.doi.org/10.1021/ic1019058 |*Inorg. Chem.* 2011, 50, 5379–5388

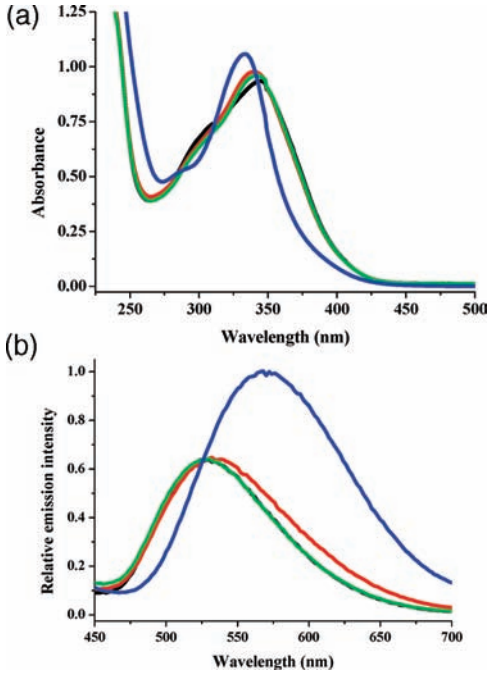

Figure 7. (a) Absorption spectra of complex **2** at a concentration of 5×10^{-5} M (black line) and in the presence of Zn^{2+} (red line), Cd^{2+} (green line), and Hg^{2+} (blue line). (b) The emission spectra of complex **2** at a concentration of 5×10^{-5} M (black line) and in the presence of Zn^{2+} (red line), Cd^{2+} (green line), and Hg^{2+} (blue line). Excitation wavelength was used at 380 nm.

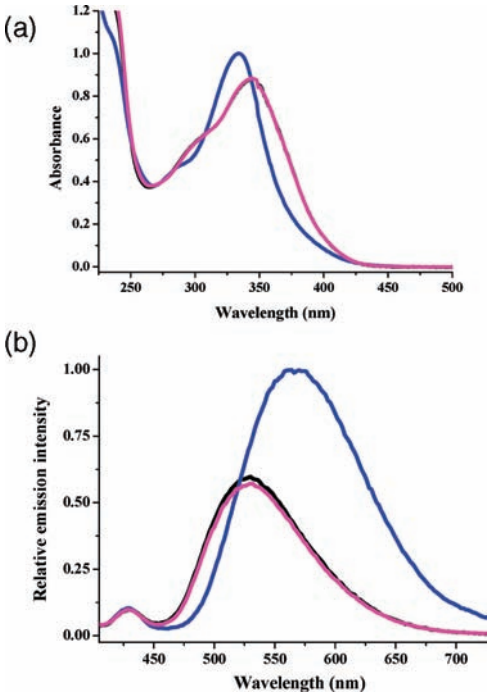

Figure 8. (a) Absorption spectra of complex **2** at a concentration of 5×10^{-5} M (black line), in the presence of 1 equiv of Hg^{2+} (blue line), and 1 equiv of [2.2.2]-cryptand added to the above solution (pink line). (b) The emission spectra of complex **2** at a concentration of 5×10^{-5} M (black line), in the presence of 1 equiv of Hg^{2+} (blue line), and 1 equiv of [2.2.2]-cryptand added to the above solution (pink line). Excitation wavelength was used at 380 nm.

band at 576 nm to be blue-shifted to 528 nm when 1−2 equiv of NaOH were added, and finally the emission was almost quenched as shown in Figure 6a. When adding HCl to a methanolic solution of complex **2**, the emission band at 528 nm was finally red-shifted to 576 nm, indicating that this pH-dependent behavior is also reversible (see Supporting Information, Figure S8). In CH_2Cl_2 (with 5% CH_3OH), addition of NaOH to a solution of complex **1** causes a direct quenching of the emission at 590 nm, and this emission is later blue-shifted to a weak one at 542 nm as shown in Figure 6b. Addition of HCl to a CH_2Cl_2 (with 5% CH_3OH) solution of complex **2** still causes the weak emission at 542 nm to red-shift and restores an enhanced emission at 590 nm (see Supporting Information, Figure S9). Therefore, distinct quenching processes depending on solvents (i.e., CH_3OH and CH_2Cl_2) have been observed. We reason that the deprotonation of the imidazole leading to the imidazolate induces an ICT process[17] to first quench the MLCT state, and then the IL state in CH_3OH. This two-step quenching process is also supported by the fact that the emission band at 538 nm for HPB in CH_3OH can be quenched during the addition of NaOH. Upon the addition of HCl to the above solution, the ICT process was blocked because of the protonation of the imidazolate to form the imidazole, and hence the MLCT emission was restored. However, the quenching process in CH_2Cl_2 (with 5% CH_3OH) seems to be a one-step process. Actually, this may be because the MLCT emission of complex **2** is more enhanced in CH_2Cl_2 (with 5% CH_3OH) compared with that in CH_3OH, and thus the quenching of the MLCT emission is dominant in the titration process and finally leaves the weak IL emission.

Group 12 Metal-Ion Recognition Studies. Since the imidazolate unit in complex **2** can act as a bridging ligand, the metal-ion binding affinity is thus evaluated for the purpose of sensing. As mentioned in the last section, complex **2** emits at 528 nm in solution, which is tentatively assigned to MLCT mixed with some IL character. Upon addition of HCl to a solution of complex **2** in CH_3OH or CH_2Cl_2 (with 5% CH_3OH), the emission band at 528 nm was finally red-shifted to 590 nm. Thus, the coordination behavior of the imidazolate unit in complex **2** may be used to examine its metal-ion sensing event. In this context, we tried to utilize the coordination preference of complex **2** toward the certain metal ions to tune its luminescent property to perform metal-ion recognition studies. Here, we set out recognition studies based on complex **2** toward group 12 metal ions (Zn^{2+}, Cd^{2+}, and Hg^{2+}),[4d] which are detected by the spectroscopic and luminescent responses.

A methanolic solution of complex **2** was titrated with a solution of Zn^{2+}, Cd^{2+}, and Hg^{2+}, respectively. Upon addition of Zn^{2+} and Cd^{2+} ions, no significant change on the absorption and luminescence spectra of complex **2** can be observed even with up to 10 equiv of ions, indicating that there is no preference for coordination toward either ion (Figure 7). However, upon addition of 1 equiv of Hg^{2+}, a blue shift (from 342 to 336 nm) and a red shift (from 528 to 570 nm) on the absorption and luminescent spectra, respectively, were observed, as shown in Figure 7. In fact, the addition of 1 equiv of Hg^{2+} to the solution of complex **2** generated the maximum shift in absorption and luminescence, which is consistent with the Job Plot (1:1, see Supporting Information, Figure S10). The above titrated spectra are quite similar to those of complex **1** (see Supporting Information, Figures S11 and S12), indicating that the imidazolate unit in

dx.doi.org/10.1021/ic1019058 |*Inorg. Chem.* 2011, 50, 5379–5388

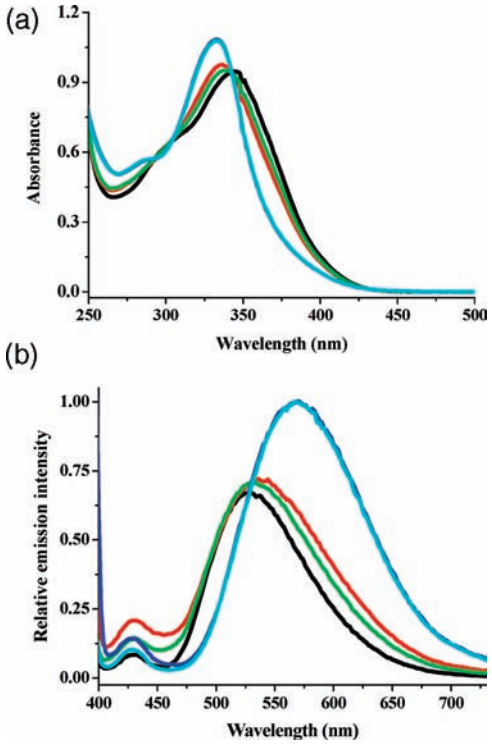

Figure 9. (a) Absorption spectra of complex **2** at a concentration of 5×10^{-5} M (black line), in the presence of 50 equiv of Zn^{2+} (red line) and Cd^{2+} (green line), and 1 equiv of Hg^{2+} added to the above solutions, respectively (blue and cyan lines). (b) The emission spectra of complex **2** at a concentration of 5×10^{-5} M (black line), in the presence of 50 equiv of Zn^{2+} (red line) and Cd^{2+} (green line), and 1 equiv of Hg^{2+} added to the above solutions, respectively (blue and cyan lines). Excitation wavelength was used at 380 nm.

the $\mathbf{2}\cdot Hg^{2+}$ adduct of **2** is very similar to the imidazole unit in **1**. A clear isosbestic point at 343 nm for the spectral trace was observed upon titration with up to 10 equiv of Hg^{2+}, and surprisingly an isoemissive point was also found at 524 nm (see Supporting Information, Figures S12−S14). A standard curve-fitting method was utilized for the A_{335} versus $Hg(ClO_4)_2$ plot to evaluate the binding constants for the 1:1 adduct ($\mathbf{2}\cdot Hg^{2+}$), and the binding constant was calculated to be 3,190 ± 60 M^{-1}.[18] Although the structural characterization regarding $\mathbf{2}\cdot Hg^{2+}$ is so far unsuccessful, its ESI mass data show the existence of the parent peak, providing some evidence for adduct formation (see Supporting Information, Figure S15). In fact, the $Hg(NO_3)_2$ has been used to examine the anion effect, and the results did show that there is no significant effect of the anions on this sensing event, that is, 566 nm for $Hg(NO_3)_2$ versus 570 nm for $Hg(ClO_4)_2$ (see Supporting Information, Figure S16).

The [2.2.2]-cryptand ligand was used to examine the reversibility of chelation of complex **2** with the Hg^{2+} ion.[19] When 1 equiv of [2.2.2]-cryptand was added to the titrated solution, the absorption and luminescent spectra were restored to the original spectra of complex **2** alone, as shown in Figure 8. Therefore, these experimental data confirm the reversible binding of complex **2** with the Hg^{2+} ion.

Finally, competing ion experiments have been also carried out, and the spectral trace is shown in Figure 9. When 50 equiv of Zn^{2+} or Cd^{2+} ions were added to a solution of complex **2**, no significant change to the absorption and luminescent spectra was observed. However, addition of 1 equiv of Hg^{2+} to the above solution generated absorption and luminescent spectra almost identical to the spectra of **2** with only Hg^{2+}. Thus, the selective sensing event of complex **2** toward Hg^{2+} among group 12 metal ions was demonstrated. We reasoned that Hg^{2+} is softer than those of Zn^{2+} and Cd^{2+}, and thus it is not unreasonable to show higher binding affinity toward the soft 2-(2′-pyridyl)-benzimidazolate ligand. That is, this can be mostly ascribed to the favorable soft−soft interaction.

CONCLUSIONS

The mononuclear Re(I) complex of 2-(2′-pyridyl)benzimidazole (**1**) has been synthesized and characterized by X-ray diffraction, and it exhibits interesting pH-dependent spectroscopic and luminescent properties. Indeed, this intriguing behavior is ascribed to the imidazole unit in complex **1**, which can be further deprotonated to form the imidazolate to give complex **2**. Addition of 1 equiv of $AuPPh_3(NO_3)$ or half an equivalent of $dppm(Au(NO_3))_2$ to complex **2** led to the formation of heteronuclear complexes **3** or **4**, respectively, with the imidazolate unit acting as a multinuclear bridging ligand. Notably, although the deprotonated methylene group coordinating to the metal ion is not unusual, the Re_2Au_4 aggregate in combination with μ_3-bridging 2-(2′-pyridyl)benzimidazolate in complex **4** is a rare example. Finally, complex **2** has been used to examine the Hg^{2+}-recognition among group 12 metal ions, and its reversibility and selectivity toward Hg^{2+} have been demonstrated.

ASSOCIATED CONTENT

Supporting Information. X-ray crystallographic CIF files for complexes **1**, $\mathbf{2}\cdot THF$, $\mathbf{3}\cdot CH_2Cl_2$, and **4** and spectroscopic data. This material is available free of charge via the Internet at http://pubs.acs.org.

AUTHOR INFORMATION

Corresponding Author

*E-mail: chebct@ccu.edu.tw (B.-C.T.), chop@ntu.edu.tw (P.-T.C), hhchang@mail.ndhu.edu.tw (A.H.-H.C.).

ACKNOWLEDGMENT

We thank the National Science Council and National Chung Cheng University of the Republic of China for financial support.

REFERENCES

(1) (a) Balzani, V.; Scandola, F. *Supramolecular Photochemistry*; Ellis Horwood: Chichester, U.K., 1991. (b) Yam, V. W.-W.; Wang, K. Z.; Wang, C. R.; Yang, Y.; Cheung, K. K. *Organometallics* **1998**, *17*, 2440. (c) Yam, V. W.-W.; Lau, V. V.-Y.; Wang, K. Z.; Cheung, K. K.; Huang, C. H. *J. Mater. Chem.* **1998**, *8*, 89.

(2) (a) Kaes, C.; Katz, A.; Hosseini, M. W. *Chem. Rev.* **2000**, *100*, 3553. (b) Balzani, V.; Juris, A.; Venturi, M.; Campagna, S.; Serroni, S. *Chem. Rev.* **1996**, *96*, 759.

(3) (a) Haga, M.-A. *Inorg. Chim. Acta* **1983**, *75*, 29. (b) Haga, M.-A.; Tsunemitsu, A. *Inorg. Chim. Acta* **1989**, *164*, 137. (c) Munakata, M.; Yan, S.-G.; Maekawa, M.; Akiyama, M.; Kitagawa, S. *J. Chem. Soc., Dalton Trans.* **1997**, 4257. (d) Chanda, N.; Sarkar, B.; Kar, S.; Fiedler, J.; Kaim, W.; Lahiri, G. K. *Inorg. Chem.* **2004**, *43*, 5128. (e) Cape, J. L.; Bowman, M. K.; Kramer, D. K. *J. Am. Chem. Soc.* **2005**, *127*, 4208. (f) Ludlow, M. K.; Soudackov, A. V.; Hammes-Schiffer, S. *J. Am. Chem. Soc.* **2009**, *131*, 7094. (g) Zeng, M. H.; Shen, X. C.; Ng, S. W. *Acta Crystallogr.* **2006**,

E62, m2194. (h) Bai, X. Q.; Zhang, S. H. *Acta Crystallogr.* **2009**, *E65*, m397.

(4) (a) Wang, K.; Huang, L.; Gao, L.; Jin, L.; Huang, C. *Inorg. Chem.* **2002**, *41*, 3353. (b) Shavaleev, N. M.; Bell, Z. R.; Easum, T. L.; Rutkaite, R.; Swanson, L.; Ward, M. D. *Dalton Trans.* **2004**, 3678. (c) Yi, H.; Crayston, J. A.; Irvine, J. T. S. *Dalton Trans* **2003**, 685. (d) Durantaye, L. D. L.; McCormick, T.; Liu, X.-Y.; Wang, S. *Dalton Trans.* **2006**, 5675.

(5) (a) Ko, S.-K.; Yang, Y.-K.; Tae, J.; Shin, I. *J. Am. Chem. Soc.* **2006**, *128*, 14150. (b) Yang, H.; Zhou, Z.; Huang, K.; Yu, M.; Li, F.; Yi, T.; Huang, C. *Org. Lett.* **2007**, *9*, 4729. (c) Shi, W.; Ma, H. *Chem. Commun.* **2008**, 1856. (d) Zhan, X.-Q.; Qian, Z.-H.; Zheng, H.; Su, B.-Y.; Lan, Z.; Xu, J.-G. *Chem. Commun.* **2008**, 1859. (e) Nolan, E. M.; Lippard, S. J. *Chem. Rev.* **2008**, *108*, 3443. (f) Santra, M.; Ryu, D.; Chatterjee, A.; Ko, S.-K.; Shin, I.; Ahn, K. H. *Chem. Commun.* **2009**, 2115.

(6) (a) Li, H.-W.; Li, Y.; Dang, Y.-Q.; Ma, L.-J.; Wu, Y.; Hou, G.; Wu, L. *Chem. Commun.* **2009**, 4453. (b) Jana, A.; Kim, J. S.; Jung, H. S.; Bharadwaj, P. K. *Chem. Commun.* **2009**, 4417. (c) Ho, M.-L.; Chen, K.-Y.; Wu, L.-C.; Shen, J.-Y.; Lee, G.-H.; Ko, M.-J.; Wang, C.-C.; Lee, J.-F.; Chou, P.-T. *Chem. Commun.* **2008**, 2438. (d) Zhao, Q.; Cao, T.; Li, F.; Li, X.; Jing, H.; Yi, T.; Huang, C. *Organometallics* **2007**, *26*, 2077.

(7) (a) *SMART, Software for the CCD Detector System*, V5.625; Bruker-AXS Instruments Division: Madison, WI, 2000. (b) *SAINT, Software for the CCD Detector System*, V6.22; Bruker-AXS Instruments Division: Madison, WI, 2000. (c) Sheldrick, G. M. *SADABS*, V 2.03; University of Göttingen: Göttingen, Germany, 2002. (d) *SHELXS-97* Sheldrick, G. M. *Acta Crystallogr.* **1990**, *A46*, 467. (e) Sheldrick, G. M. *SHELXL-97*; University of Göttingen: Göttingen, Germany, 1997.

(8) (a) Becke, A. D. *J. Chem. Phys.* **1993**, *98*, 5648. (b) Lee, C.; Yang, W.; Parr, R. G. *Phys. Rev. B* **1988**, *37*, 785. (c) Hay, P. J.; Wadt, W. R. *J. Chem. Phys.* **1985**, *82*, 299.

(9) Frisch, M. J.; Trucks, G. W.; Schlegel, H. B.; Scuseria, G. E.; Robb, M. A.; Cheeseman, J. R.; Montgomery, J. A., Jr.; Vreven, T.; Kudin, K. N.; Burant, J. C.; Millam, J. M.; Iyengar, S. S.; Tomasi, J.; Barone, V.; Mennucci, B.; Cossi, M.; Scalmani, G.; Rega, N.; Petersson, G. A.; Nakatsuji, H.; Hada, M.; Ehara, M.; Toyota, K.; Fukuda, R.; Hasegawa, J.; Ishida, M.; Nakajima, T.; Honda, Y.; Kitao, O.; Nakai, H.; Klene, M.; Li, X.; Knox, J. E.; Hratchian, H. P.; Cross, J. B.; Bakken, V.; Adamo, C.; Jaramillo, J.; Gomperts, R.; Stratmann, R. E.; Yazyev, O.; Austin, A. J.; Cammi, R.; Pomelli, C.; Ochterski, J. W.; Ayala, P. Y.; Morokuma, K.; Voth, G. A.; Salvador, P.; Dannenberg, J. J.; Zakrzewski, V. G.; Dapprich, S.; Daniels, A. D.; Strain, M. C.; Farkas, O.; Malick, D. K.; Rabuck, A. D.; Raghavachari, K.; Foresman, J. B.; Ortiz, J. V.; Cui, Q.; Baboul, A. G.; Clifford, S.; Cioslowski, J.; Stefanov, B. B.; Liu, G.; Liashenko, A.; Piskorz, P.; Komaromi, I.; Martin, R. L.; Fox, D. J.; Keith, T.; Al-Laham, M. A.; Peng, C. Y.; Nanayakkara, A.; Challacombe, M.; Gill, P. M. W.; Johnson, B.; Chen, W.; Wong, M. W.; Gonzalez, C.; Pople, J. A. *Gaussian 03*, Revision E.01; Gaussian, Inc.: Wallingford, CT, 2004.

(10) Janiak, C. *Dalton Trans.* **2003**, 2781.

(11) (a) Feng, D.-F.; Tang, S. S.; Liu, C. W.; Lin, I. J. B.; Wen, Y.-S.; Liu, L.-K. *Organometallics* **1997**, *16*, 901. (b) Usón, R.; Laguna, A.; Laguna, M.; Lázaro, I.; Jones, P. G. *Organometallics* **1987**, *6*, 2326. (c) Usón, R.; Laguna, A.; Laguna, M.; Gimeno, M. C.; Jones, P. G.; Fittschen, C.; Sheldrick, G. M. *J. Chem. Soc., Chem. Commun.* **1986**, 509.

(12) Brown, R. G.; Eniwlstle, N.; Hepworth, J. D.; Hodgson, K. W.; Bernadette, M. *J. Phys. Chem.* **1982**, *86*, 2418.

(13) Rath, M. C.; Palit, D. K.; Mukherjee, T. *J. Chem. Soc., Faraday Trans.* **1998**, *94* (9), 1189.

(14) (a) Che, C.-M.; Kwong, H.-L.; Yam, V.W.-W.; Cho, K.-C. *J. Chem. Soc., Chem. Commun.* **1989**, 885. (b) Fu, W.-F.; Chan, K.-C.; Miskowski, V. M.; Che, C.-M. *Angew. Chem., Int. Ed.* **1999**, *38*, 2783.

(15) King, C.; Wang, J. C.; Khan, M. N. I.; Fackler, J. P., Jr. *Inorg. Chem.* **1989**, *28*, 2145.

(16) Chou, P.-T.; Chi, Y. *Chem.—Eur. J.* **2007**, *13*, 380.

(17) (a) Saha, S.; Samanta, A. *J. Phys. Chem. A* **1998**, *102*, 10579. (b) Sarkar, M.; Banthia, S.; Patil, A.; Ansari, M. B.; Samanta, A. *New. J. Chem.* **2006**, *30*, 1557.

(18) Connors, K. A. *Binding Constants*; John Wiley and Sons: New York, 1987.

(19) Harano, K.; Hiraoka, S.; Shionoya, M. *J. Am. Chem. Soc.* **2007**, *129*, 5300.